Coupled Bistable Chemical Systems – Experimental Realization of Boolean Functions Using a Simple Feedforward Net

K.-P. Zeyer, G. Dechert, W. Hohmann, R. Blittersdorf, and F. W. Schneider

Institut für Physikalische Chemie der Universität Würzburg, Marcusstraße 9–11, D-97070 Würzburg, Germany

Z. Naturforsch. **49a**, 953–963 (1994); received May 28, 1994

We use the BZ-reaction and the MBO-reaction to implement the Boolean functions AND, OR, NAND, and NOR by the coupling of three chemical reactors. The experimental setup is analogous to a simple neural feedforward network with two reactors serving as the input layer and one reactor as the output layer. Coupling between the input and output reactors is carried out through the flow rate (BZ- and MBO-reaction) and through the electrical current by the use of Pt working electrodes (BZ-reaction). The XOR- and XNOR functions may be realized with 5 reactors using combinations of the AND, NOR, NOR- and the AND, NOR, Or-chemical gates, respectively.

Key words: Nonlinear systems; Flow-rate-coupling; Electrical coupling; Neural nets; Boolean functions.

1. Introduction

Coupled nonlinear chemical reactions may serve as models for aspects of coupling in living cells and tissues, and neural nets [1]. A number of experimental studies on coupled homogeneous nonlinear chemical reactions deals with feedback processes [2–9] or the coupling of two reactors through mass exchange [10–12], by common species [22–24], electrochemically [25, 26], or by flow rate [27–29]. Experimental mass coupling of three reactors has been investigated in batch reactors [30] and under flow conditions [31] in a triangular arrangement. Linear arrays of mass coupled reactors, each operating in a bistable mode, were explored by Stuchl and Marek [32] using up to 7 reactors and Laplante and Erneux [33] using 16 reactors. Stuchl and Marek [32] obtained different combinations of the two possible steady states by perturbing one reactor with ceric or bromide ions. Their results therefore resemble binary information coding [32]. Laplante and Erneux [33] studied the speed of a propagation wave with respect to coupling strength.

Recently, the realization of neural networks with computing abilities using coupled nonlinear chemical systems was described theoretically [34–36]. Hjelmfelt and Ross [37] and Hjelmfelt, Schneider, and Ross [38] investigated a Hopfield like network of mass coupled reactors consisting of up to 72 systems. The network can be programmed with different binary patterns of a bistable reaction using Hebb's learning rule [39], which determines the connections between the reactors [37, 38]. The programmed net is capable to recognize patterns similar to the stored patterns [37, 38].

In this work we present experiments which express the Boolean functions: AND, OR, NAND, and NOR using the Minimal-Bromate-Oscillator (MBO)-system [40, 41] with flow-rate-coupling and the Belousov-Zhabotinskii (BZ)-reaction [42, 43] with flow-rate-coupling and electrical coupling. Recently, these logical functions were carried out chemically by using a neutralization reaction [44].

2. Experimental

The flow-rate-coupling experiments on the BZ-reaction and the MBO-system (Fig. 1 a) consist of three separate CSTRs (7.6 ml volume for each CSTR in BZ-experiments and 3.5 ml for each reactor in MBO-experiments) coupled in the same way.

The setup for the electrical coupling in the BZ-reaction is shown in Figure 1 b. This arrangement is similar to the flow-rate-coupling experiments but requires three additional reference reactors filled with a Ce^{3+}/Ce^{4+}-mixture (9:1) and electrical contact to close the electrical circuits. Permeability between working and reference reactor of each couple is guaranteed by teflon membranes (1–2 μm pore size) at both ends of the salt bridge. Mass exchange is prevented by the constant flow of sulfuric acid solution inside the salt bridge [25].

Reprint requests to Prof. Dr. F. W. Schneider.

0932-0784 / 94 / 1000-0953 $ 06.00 © – Verlag der Zeitschrift für Naturforschung, D-72027 Tübingen

Each pair of reactors is connected via Pt working electrodes to a potentiostat supplying a potential. The electrodes in the working reactors always serve as cathodes. Potential changes of the BZ-reaction are registered with a Pt/Ag/AgCl reference electrode inserted in the working reactors.

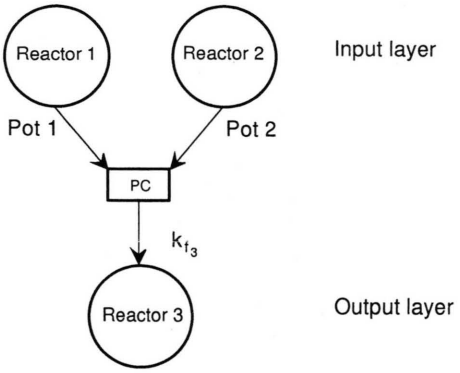

Fig. 1a. Flow-rate-coupling experiments: Reactors 1 and 2 serve as the input while reactor 3 is the output. Exchange of reaction solutions does not occur between the reactors. Coupling proceeds from reactor 1 to 3 and 2 to 3 via the flow rate according to (1). Pot1 and pot2 are voltages which are proportional to the measured redox potential. PC: personal computer which converts the input signals (pot1 and 2) to flow rates into reactor 3.

In all setups the coupling of the CSTRs resembles a simple feedforward net. Feedforward nets are arranged in at least two layers (input and output layer). The input layer is used to give activation to the system. The activation of the input layer neurons is processed forward to the next layer (hidden or output layer) using defined links. These links correspond to the axons with dentrites and synapses in biological neural networks [45]. They are modeled by linear functions in feedforward nets. In the flow-rate-coupling experiments the output signals of reactor 1 and 2 are transformed into a flow rate which is applied to reactor 3 using the following linear equation:

$$k_{f3} = k_{f\,min} + W_{13} \cdot \text{pot1} + W_{23} \cdot \text{pot2} + B_3 \quad (1)$$

with a) $k_{f\,min} = 2.50 \cdot 10^{-5}\ s^{-1}$, (BZ)
b) $k_{f\,min} = 3.00 \cdot 10^{-5}\ s^{-1}$, (MBO)

where the values of pot1 [mV] and pot2 [mV] are proportional to the redox potentials measured by a Pt-electrode in each reactor. The redox potentials are mainly related to the ceric/cerous ion ratio [25, 46] in the BZ-reaction and the MBO-system. These values are recorded every second and simultaneously converted according to (1). The quantities W_{13} [$s^{-1}\,mV^{-1}$]

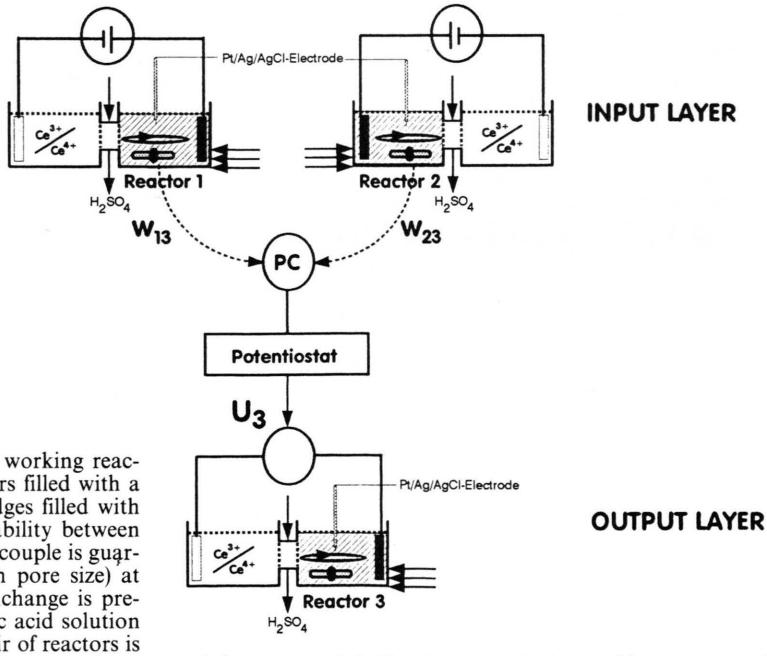

Fig. 1b. Electrical coupling: All three working reactors are connected to reference reactors filled with a Ce^{3+}/Ce^{4+}-mixture (9:1) via salt bridges filled with sulfuric acid solution (1.5 M). Permeability between working and reference reactor of each couple is guaranteed by teflon membranes (1–2 μm pore size) at both ends of the salt bridge. Mass exchange is prevented by the constant flow of sulfuric acid solution inside the salt bridge [25, 48]. Each pair of reactors is connected via Pt working electrodes to a potentiostat supplying a potential. The electrodes in the working reactors always serve as cathodes. Potential changes of the BZ-reaction are registered with a Pt/Ag/AgCl reference electrode inserted in the working reactors. Working reactors 1 and 2 serve as the input while reactor 3 is the output. Coupling proceeds from reactor 1 to 3 and 2 to 3 via a variable potential U_3 applied to reactor 3 according to Equation (2).

and W_{23} [$s^{-1}\,mV^{-1}$] represent the coupling strengths between each input reactor and the output reactor, and B_3 [s^{-1}] is a bias parameter. The results are transformed to analog signals via a 12 bit digital/analog converter card and then converted to a frequency. The resulting frequency is applied to the stepping motor of the linear feed pump of reactor 3 (Table 1). Values smaller than $k_{f\,min}$ resulting from (1) are set to the smallest possible flow rate $k_{f\,min}$ of our setups.

In the case of electrical coupling the measured redox potentials of reactor 1 and 2 are transformed according to:

$$U_3 = w_{13} \cdot \text{pot1} + w_{23} \cdot \text{pot2} + b_3 \,. \qquad (2)$$

The functions pot1 [mV] and pot2 [mV] are the measured potentials in the input reactors 1 and 2. The dimensionless parameters w_{13} and w_{23} are connectivities chosen appropriate for the individual logical functions (Table 2); b_3 [mV] is a bias parameter. The results are converted via a 12 bit digital/analog converter board and then given to a potentiostat. U_3 [mV] denotes the potential applied to the output reactor by the potentiostat via Pt working electrodes.

Each reactor works in a bistable parameter range of the BZ-reaction and the MBO-system. De Kepper, Rossi, and Pacault [47] characterized conditions for which the BZ-reaction shows bistability. Dechert and Schneider [48] elaborated a set of parameters to investigate the influence of perturbations by electrode processes in a bistable range of the BZ-reaction.

Table 1. The experimental connectivities W_{ij} [$mV^{-1}\,s^{-1}$] and the bias values B_3 [s^{-1}] for the Boolean functions AND, OR, NAND, NOR in the flow-rate-coupled BZ-reaction.

	AND	OR	NAND	NOR
W_{13}	1.6e−05	1.6e−05	−1.6e−05	−1.6e−05
W_{23}	1.6e−05	1.6e−05	−1.6e−05	−1.6e−05
B_3	−1.4e−02	−9.1e−03	1.8e−02	1.2e−02

Table 2. The experimental connectivities w_{ij} [dimensionless] and the bias values b_3 [mV] for the Boolean functions AND, OR, NAND, NOR in the electrically coupled BZ-reaction.

	AND	OR	NAND	NOR
w_{13}	−3.48	−1.74	1.74	3.48
w_{23}	−3.48	−1.74	1.74	3.48
b_3	4031	2030	−696	−1392

In the case of electrical coupling the flow rates in all three working reactors are kept constant at $k_f = 1.7 \cdot 10^{-3}\,s^{-1}$. At this flow rate the system stays on the kinetic branch above the bistable region (Figure 2a).

Bistability in the MBO was reported first by Geiseler et al. [49]. Guided by this work we determined a set of suitable concentrations for a bistable region of the MBO-system. Each reactor is fed with three feed-streams containing the following solutions:

BZ-reaction (flow-rate-coupling and electrical coupling):

I:	$6.0 \cdot 10^{-3}$	mol/l	$KBrO_3$
II:	$2.0 \cdot 10^{-3}$	mol/l	Ce^{3+} from $Ce_2(SO_4)_3$
	0.10	mol/l	$HOOCCH_2COOH$
III:	4.5	mol/l	H_2SO_4

MBO-system:

I:	0.135	mol/l	$KBrO_3$
II:	$9.0 \cdot 10^{-4}$	mol/l	Ce^{3+} from $Ce_2(SO_4)_3$
	$5.4 \cdot 10^{-3}$	mol/l	KBr
III:	3.0	mol/l	H_2SO_4 .

To obtain reactor concentrations divide by 3. The malonic acid was recrystallized twice from acetone to remove trace impurities [50]. All other chemicals are of analytical grade and used without further purification. All solutions are prepared from water purified by ion exchange (specific resistance $>10\,M\Omega \cdot cm$; purification system Milli-Q, Millipore). The reactors in both experimental setups are stirred magnetically with teflon stirrers at 800 r.p.m. The flow rates of the above solutions into the three reactors are regulated separately with three precise linear pumps. The reactors, feed-lines, and syringes are thermostated at $25 \pm 0.2\,°C$.

In the above parameter range the BZ-system displays a low redox potential for low flow rates (thermodynamic branch) [48]. When the flow rate is increased, the steady-state looses stability at $k_f = 0.0014\,s^{-1}$ and produces a new steady state with a higher potential (kinetic branch). Decreasing the flow rate, the system returns to the low-potential branch at $k_f = 0.0008\,s^{-1}$ displaying the phenomenon of hysteresis. Between these flow rates the BZ-reaction shows bistability (Figure 2a).

At a constant flow rate above bistability the application of electrical current induces switching between the kinetic branch and a lower steady state. This transi-

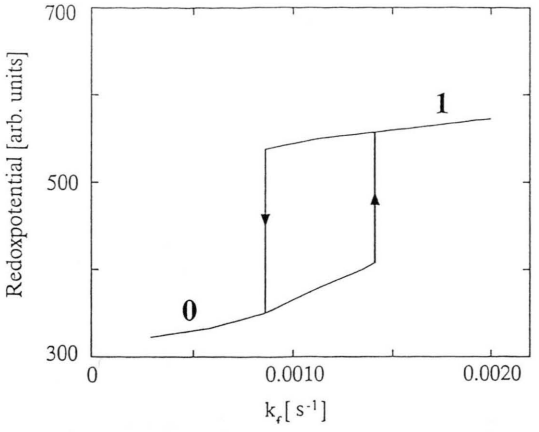

Fig. 2a. Bifurcation diagram of the experimental BZ-reaction (schematic representation). At low flow rates, low-potential (thermodynamic branch) steady states ("0") exist, whereas at high flow rates the system switches to high-potential (kinetic branch) steady states ("1"). In the flow rate interval from $k_f = 0.0008\ s^{-1}$ to $k_f = 0.0014\ s^{-1}$ the BZ-reaction shows bistability. The arrows indicate transitions leading to hysteresis.

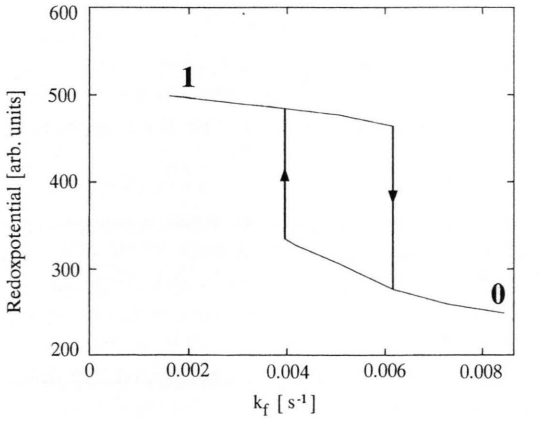

Fig. 2b. Bifurcation diagram of the experimental MBO-system in the parameter range for bistability (schematic representation). Bistability occurs in the flow rate interval from $k_f = 4.0 \cdot 10^{-3}\ s^{-1}$ to $k_f = 6.0 \cdot 10^{-3}\ s^{-1}$. Notice that in the MBO-system the thermodynamic and kinetic branches are reversed with respect to the BZ-reaction (Figure 2a).

tion occurs only above a threshold value of the potential [48]. This offers an additional chemical switch sufficient for the implementation of Boolean logical functions.

In the corresponding parameter range the MBO-system (Fig. 2b) shows bistability with a high redox potential at low flow rates (thermodynamic branch) and a low potential kinetic branch at high flow rates. The switching between states occurs for $k_f = 6.0 \cdot 10^{-3}\ s^{-1}$ with increasing flow rate and for $k_f = 4.0 \cdot 10^{-3}\ s^{-1}$ decreasing flow rate.

3. Logical Functions

We consider a special case of Boolean algebra with only two elements denoted as "0" and "1". Assume that a and b are Boolean variables and the values of these variables can either be "0" or "1". Connections are described by the Boolean functions f_b. The simplest connection is the identity $f_b(a) = a$ and the negation $f_b(a) = \bar{a}$ working with one or more arguments.

On the other hand, the functions AND, OR, NAND, and NOR require two or more arguments, where AND is denoted by $f_b(a, b) = a \wedge b$. The result of this function is "1" if both arguments are "1". Otherwise the result is always "0". The OR-function is $f_b(a, b) = a \vee b$. The result "1" is obtained if both or at least one of the arguments are "1". The NAND- and NOR-connections are the negations of the AND- and the OR-functions.

The XOR-function (exclusive OR) and its negation XNOR represent composed Boolean functions, which are denoted as

$$f_b(a, b) = \overline{(a \wedge b) \vee \overline{(a \vee b)}}$$

and

$$f_b(a, b) = (a \wedge b) \vee \overline{(a \vee b)}, \quad \text{respectively.}$$

This shows that the XOR-function is composed of one AND- and two NOR-connections. The XNOR-connection is a combination of one AND-, one NOR-, and one OR-function.

The XOR-function gives the result "1" only if both arguments are different, while the XNOR-function yields "1" if both arguments are equal. The XOR- and XNOR-gate can be implemented chemically using 5 coupled reactors: Two reactors serve as the input layer, two reactors as the hidden layer, and one reactor as the output layer in a neural feedforward net [51].

4. Results

4.1. BZ-reaction

We arbitrarily denote all monostable steady states below the bistable region as "0" ($k_f < 0.0008\ s^{-1}$) and the steady states above the bistable region as "1" ($k_f > 0.0014\ s^{-1}$).

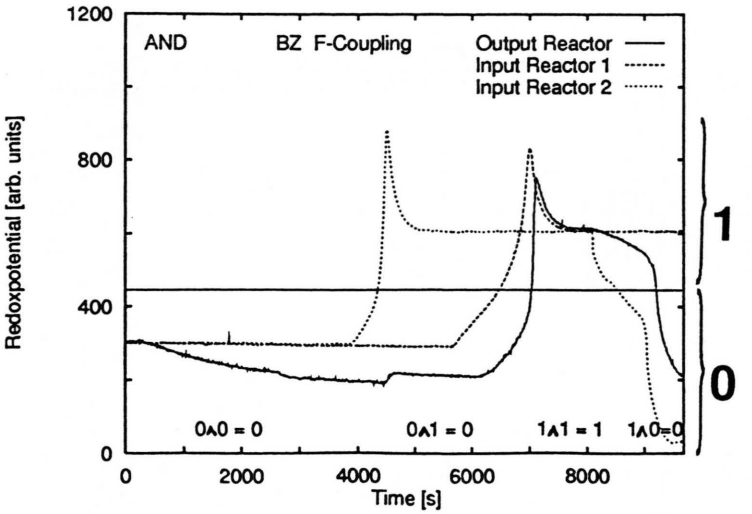

Fig. 3. The logical AND-function with flow-rate-coupling in the BZ-reaction: Experimental redox potential versus time. Both input reactors are initially in the "0" state. The following combinations are shown: $0 \wedge 0 = 0$, $0 \wedge 1 = 0$, $1 \wedge 1 = 1$, and $1 \wedge 0 = 0$. All states above 450 arb. units (solid line) are denoted as "1" and below 450 arb. units as "0" (see Figure 2a). Large overshoots are observed.

a) Flow-rate-coupling

At the beginning of each experiment, the input reactors are allowed to assume the state "0" ($k_f = 4.54 \cdot 10^{-4}$ s^{-1}) or state "1" ($k_f = 3.6 \cdot 10^{-3}$ s^{-1}). Before the coupling process is started, the output reactor 3 is always set to "0" ($k_f = 4.54 \cdot 10^{-4}$ s^{-1}). After initiating the flow-rate-coupling, reactor 3 assumes a steady state according to the particular Boolean function used. The appropriate connectivities (Table 1) were tested with the four possible input combinations 00, 10, 01, and 11.

The AND-function is shown in Figure 3. Initially both input reactors are set to "0". After coupling (1) has been started, the output remains in the "0" state. After reactor 2 has been switched to the "1" state, the output remains "0". When both input reactors are converted to the "1" state, the output changes to "1". When reactor 2 is changed to the "0" state, the output reactor changes to "0" with a time delay.

During the switching processes, overshoots emerge when the system changes from the low- to the high-potential branch. Undershoots in the potential take place in the reverse case. The chemical OR-gate is demonstrated in Figures 4a, b. The OR-function leads to the result "1" if at least one of the inputs is "1".

The negation of the AND-function (NAND) is represented in Figures 5a, b. The output is always "1" except if the input "1" is applied in both reactors. The NOR-gate (Fig. 6) leads only to the result "1" if both inputs are in the "0" state.

b) Electrical Coupling

During the electrical coupling experiments, all flow rates ($k_f = 1.7 \cdot 10^{-3}$ s^{-1}) in the three working reactors are kept constant. At this flow rate the kinetic branch (state "1") is stable at zero potential. Transitions from the kinetic branch to a steady state of a lower potential in the input reactors are induced by superthreshold potentials (≥ 960 mV) externally applied. The lower steady state is only stable during current flow, and the system returns on the kinetic branch if the potential is reduced below a threshold. All possible combinations of "0" and "1" are realized in the described way in the input reactors. The potential U_3 is evaluated according to (2) and applied to the output reactor. The connectivities w_{13}, w_{23} and the bias b_3 are given in Table 2. The Figs. 7–10 show the AND-, OR-, NAND-, and NOR-function.

4.2. MBO-system

In the bistability region of the MBO-system the high-potential branch at low flow rates ($k_f < 4.0 \cdot 10^{-3}$ s^{-1}) is denoted as "1" whereas the low-potential branch at higher flow rates ($k_f > 6.0 \cdot 10^{-3}$ s^{-1}) is named "0". This situation is contrary to the one in the bistability region of the BZ-reaction, as seen in Figs. 2a and 2b.

The AND-gate is shown in Figure 11. Initially both input reactors are set to "0", so the output reactor also stays in the "0" state. When one of the input reactors

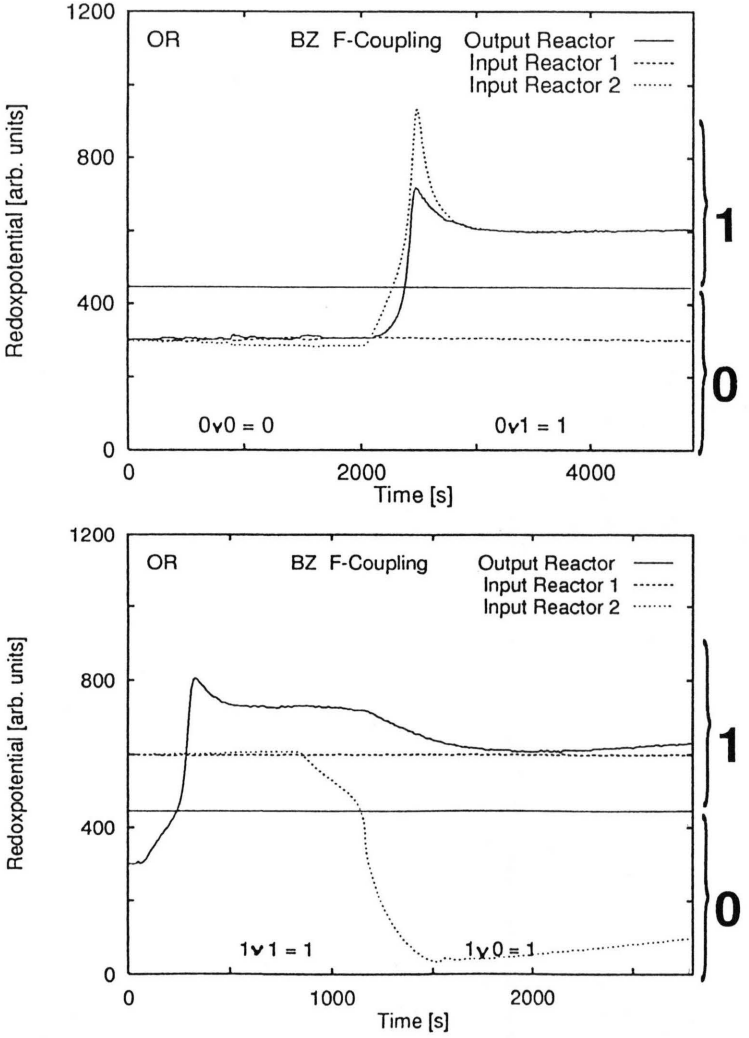

Fig. 4. The OR-function with flow-rate-coupling in the BZ-reaction. a) The combinations $0 \vee 0 = 0$ and $0 \vee 1 = 1$ are shown. b) The two remaining combinations $1 \vee 1 = 1$ and $1 \vee 0 = 1$ are shown. When reactor 2 is switched to a low potential state ("0") the output decreases somewhat due to a relatively large decrease in k_{f3}, but it remains "1". A mild potential undershoot is observed.

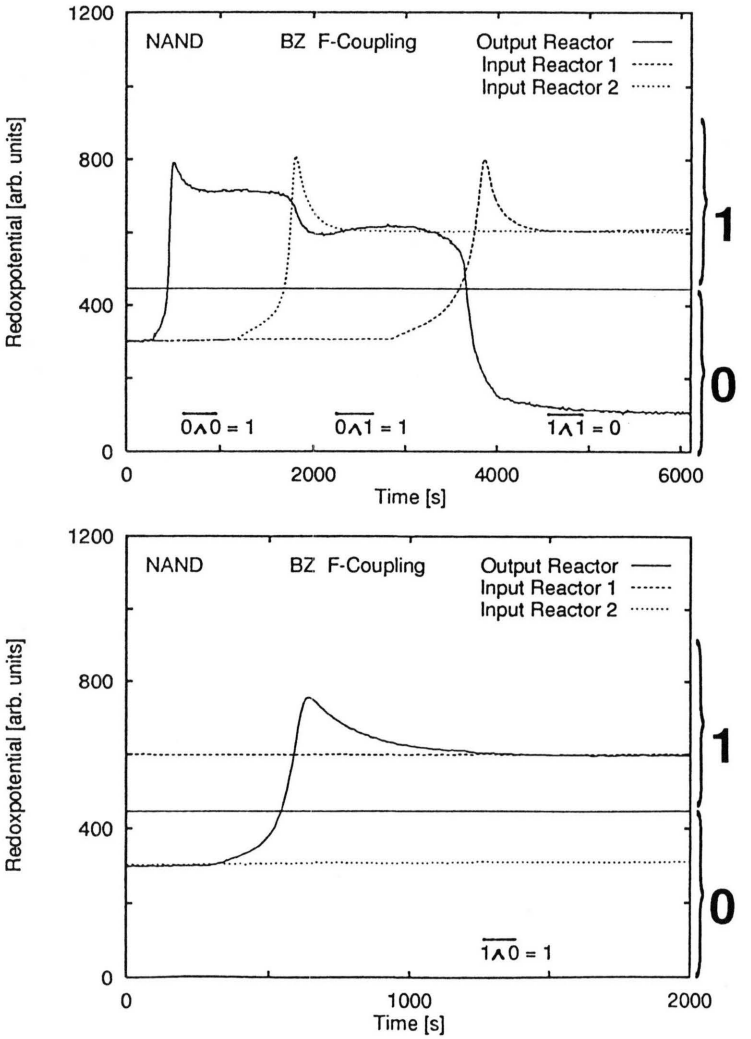

Fig. 5. The NAND-function with flow-rate-coupling in the BZ-reaction. a) The following combinations are shown: $\overline{0 \wedge 0} = 1$, $\overline{0 \wedge 1} = 1$, and $\overline{1 \wedge 1} = 0$. b) The remaining combination $\overline{1 \wedge 0} = 1$ is shown.

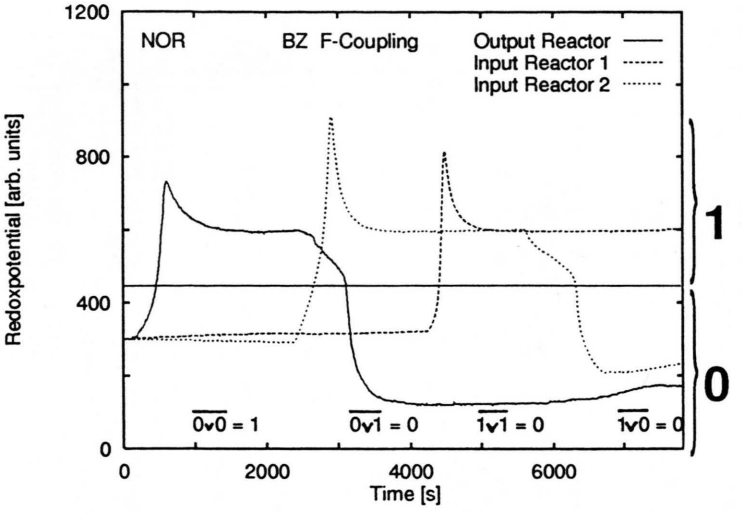

Fig. 6. The NOR-function with flow-rate-coupling in the BZ-reaction for all 4 input combinations: $\overline{0 \vee 0} = 1$, $\overline{0 \vee 1} = 0$, $\overline{1 \vee 1} = 0$, and $\overline{1 \vee 0} = 0$.

Table 3. The experimental connectivities W_{ij} [$mV^{-1} s^{-1}$] and bias values B_3 [s^{-1}] for the Boolean functions AND, OR, NAND, and NOR in the flow-rate-coupled MBO-system.

	AND	OR	NAND	NOR
W_{13}	−3.07e−05	−3.07e−05	3.07e−05	3.07e−05
W_{23}	−3.07e−05	−3.07e−05	3.07e−05	3.07e−05
B_3	3.27e−02	2.56e−02	−2.16e−02	−1.45e−02

Table 4. The experimental W_{ij} [$mV^{-1} s^{-1}$] and B_j [s^{-1}] values for the Boolean functions XOR with the four possible combinations 0 XOR 0 = 0, 0 XOR 1 = 1, 1 XOR 0 = 1, and 1 XOR 1 = 0 and XNOR with the combinations 0 XNOR 0 = 1, 0 XNOR 1 = 0, 1 XNOR 0 = 0, and 1 XNOR 1 = 1 in the flow-rate-coupled BZ-reaction.

	XOR	XNOR
W_{13}	1.6e−05	1.6e−05
W_{23}	1.6e−05	1.6e−05
B_3	−1.4e−02	−1.4e−02
W_{14}	−1.6e−05	−1.6e−05
W_{24}	−1.6e−05	−1.6e−05
B_4	1.2e−02	1.2e−02
W_{35}	−1.6e−05	1.6e−05
W_{45}	−1.6e−05	1.6e−05
B_5	1.1e−02	−8.8e−03

is set to "1", the output reactor remains in state "0". Only for both input reactors in state "1" the output reactor finally switches to "1". In a similar way the OR-, NAND-, and NOR-functions are shown in Figs. 12, 13, and 14. The connectivities are listed in Table 3.

The XOR-function can be implemented with both systems by using 5 reactors. For input and hidden layers a combination of the AND- and NOR-functions is employed, and the connection between the hidden layer and the output layer is represented by a NOR-gate [51]. Alternatively, we used the known solutions of the AND- and NOR-gates and applied them as the input into a NOR-function to simulate the XOR-gate (not shown). Using an OR-function in the last step, the XNOR-connection was also implemented. The experimentally used connectivities for flow-rate-coupling in the BZ-reaction appropriate for solving the XOR- and XNOR-function are given in Table 4.

5. Discussion

The "0" and "1" states represent a range of steady states located on the low-potential and high-potential branches, respectively. The redox potential changes relatively rapidly for both systems and coupling methods when the coupling is initiated. The connectivities have been chosen in both sets of flow-rate-coupling in order that the resulting flow rates into reactor 3 are outside the bistable steady state region. Therefore the purpose of the bistability is to serve as a chemical switch.

In the electrical coupling experiments the switching between the kinetic branch and a lower potential steady state occurs through a cathodic potential causing the reduction of the Ce^{4+} to Ce^{3+} on the Pt

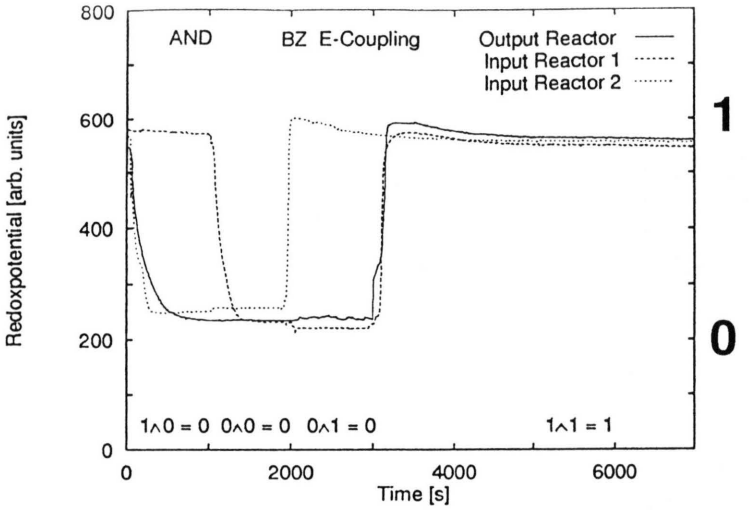

Fig. 7. The AND-function realized in the BZ-reaction with electrical coupling at a constant flow rate $k_f = 1.7 \cdot 10^{-3}\,s^{-1}$. All 4 possible combinations $1 \wedge 0 = 0, 0 \wedge 0 = 0, 0 \wedge 1 = 0$, and $1 \wedge 1 = 1$ are shown. The stable kinetic branch represents state "1" (see Fig. 2a). State "0" is obtained when a potential above the threshold (≥ 960 mV) is applied to the system on the kinetic branch. Over- or undershoots are not observed here.

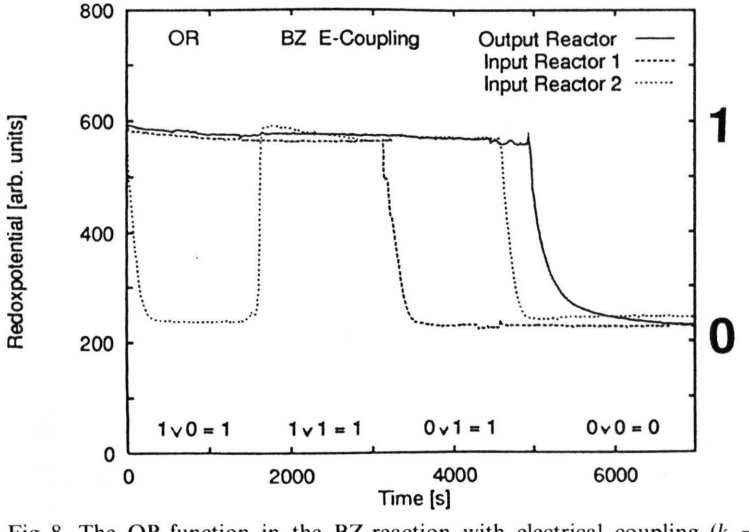

Fig. 8. The OR-function in the BZ-reaction with electrical coupling ($k_f = 1.7 \cdot 10^{-3}\,s^{-1}$). All 4 possible combinations $1 \vee 0 = 1, 1 \vee 1 = 1, 0 \vee 1 = 1$, and $0 \vee 0 = 0$ are shown.

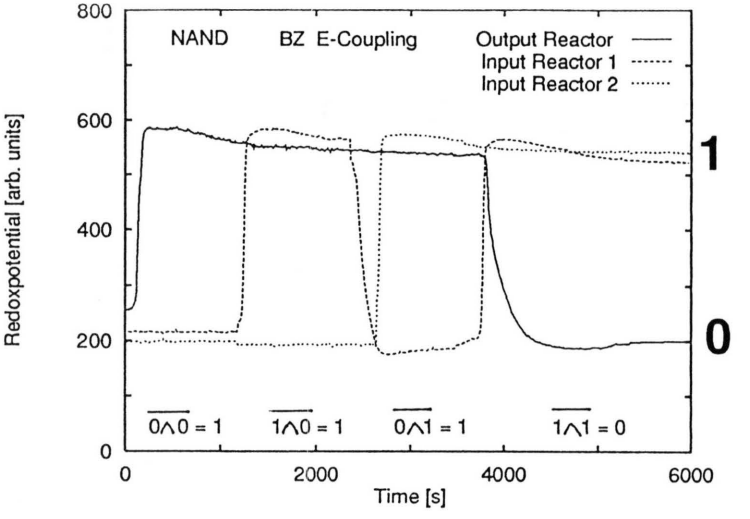

Fig. 9. The NAND-function in the BZ-reaction with electrical coupling. All 4 possible combinations $\overline{0 \wedge 0} = 1$, $\overline{1 \wedge 0} = 1$, $\overline{0 \wedge 1} = 1$, and $\overline{1 \wedge 1} = 0$ are shown.

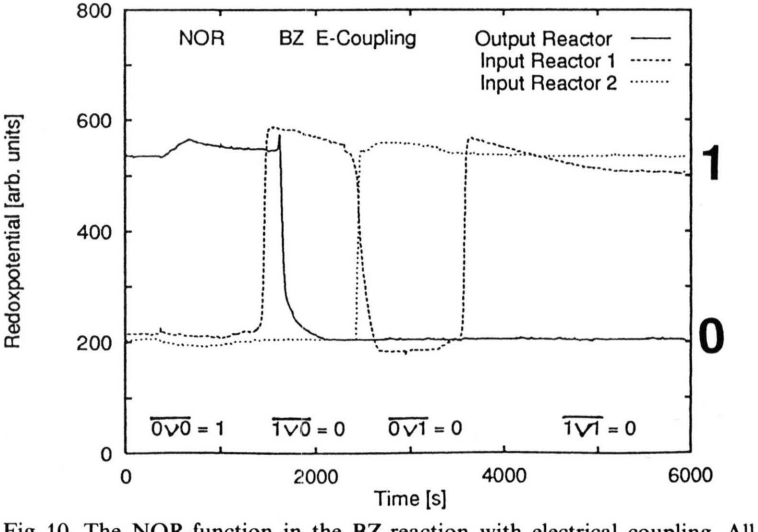

Fig. 10. The NOR-function in the BZ-reaction with electrical coupling. All 4 possible combinations $\overline{0 \vee 0} = 1$, $\overline{1 \vee 0} = 0$, $\overline{0 \vee 1} = 0$, and $\overline{1 \vee 1} = 0$ are shown.

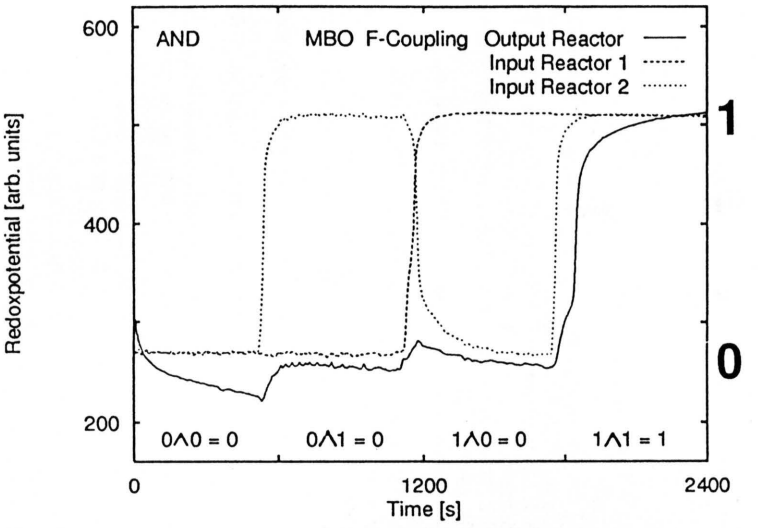

Fig. 11. The experimental AND-function in the flow-rate-coupled MBO-system. Redox potential versus time. The following combinations are shown $0 \wedge 0 = 0$, $0 \wedge 1 = 0$, $1 \wedge 0 = 0$, and $1 \wedge 1 = 1$.

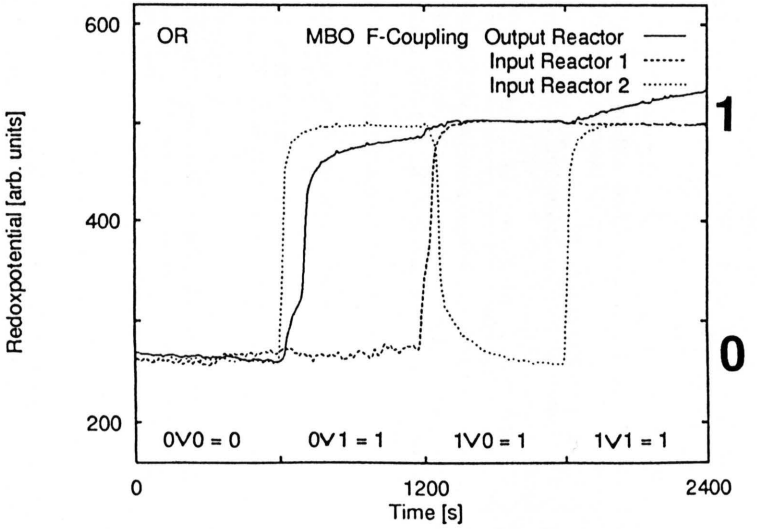

Fig. 12. The experimental OR-function in the flow-rate coupled MBO-system. All 4 possible combinations $0 \vee 0 = 0$, $0 \vee 1 = 1$, $1 \vee 0 = 1$, and $1 \vee 1 = 1$ are shown.

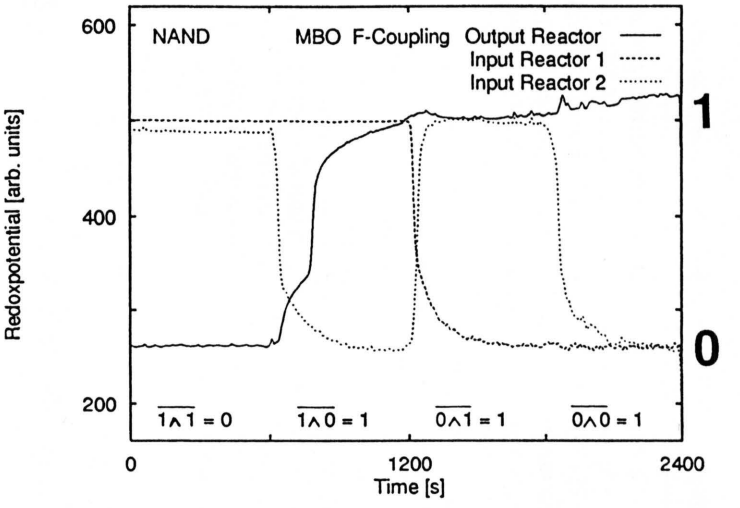

Fig. 13. The experimental NAND-function in the flow-rate-coupled MBO-system. The following combinations are shown $\overline{1 \wedge 1} = 0$, $\overline{1 \wedge 0} = 1$, $\overline{0 \wedge 1} = 1$, and $\overline{0 \wedge 0} = 1$.

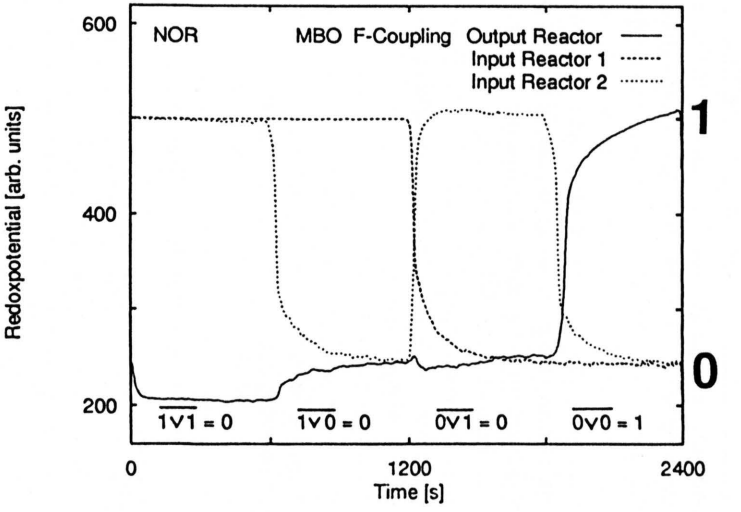

Fig. 14. The experimental NOR-function in the flow-rate-coupled MBO-system. The following combinations are shown $\overline{1 \vee 1} = 0$, $\overline{1 \vee 0} = 0$, $\overline{0 \vee 1} = 0$, and $\overline{0 \vee 0} = 1$.

working electrode. In the flow-rate-coupling of the BZ-reaction a large overshoot is observed in the redox potential when a transition from the thermodynamic to the kinetic branch occurs. Switching in the opposite direction undershoots the lower steady state, as observed in Figures 3, 4, and 6. Over- and undershoots are well known from transition studies in the BZ-reaction [32] and in other nonlinear reactions in bistable parameter ranges [52–54]. There are no over- or undershoots observed in the MBO-system when transitions between the two states take place. Switching between steady states by flow-rate-coupling proceeds faster in the MBO, since the MBO is a pure flow-system. The MBO-reaction requires higher flow rates to observe comparable behaviour as in the BZ-reaction. The electrical coupling transitions between steady states are more rapid than those in flow-rate-coupling. Electrode processes involve mainly the cerium redox couple [25, 46], whereas flow-rate-coupling involves all species.

The Oregonator model [55] predicts bistability for the BZ-reaction, however, its thermodynamic and kinetic branches are reversed with respect to the BZ-experiments (Figure 2a). Other models based on the Oregonator [56, 57] have not yet been sufficiently tested numerically to yield regions of bistability that agree with the present experiments. For the MBO we [51] have simulated the Boolean functions by the use of a bistability range in a modified Noyes-Field-Thompson (NFT) model [40, 58] in good agreement with experiment.

Our experimental arrangement resembles a simple feedforward net to realize the logical gates AND, OR, NAND, NOR, XOR, and XNOR. Large networks with computing abilities have been suggested but their experimental realization suffers from the experimental handling of many connectivities [37, 38]. Other bistable reactions which show relatively sharp transitions between two states are suitable for constructing logical gates. The simple Boolean functions can be combined, and more complex devices such as adding machines should be constructable. Our experimental systems are hybrid devices using a chemical reaction and a conventional computer to calculate the flow rates and electrical potentials. It would be desirable to construct a chemical network that self-adjusts its connectivities.

Acknowledgement

We thank the Deutsche Forschungsgemeinschaft and the Volkswagenstiftung for financial support and D. Lebender for valuable discussions. We also thank E. Ullmann and J. Zimmermann for the construction of the reactor and the implementation of electronic data control.

[1] M. Marek and I. Schreiber, Chaotic Behaviour of Deterministic Dissipative Systems. Academia, Prag 1991, p. 221, and references therein.
[2] A. M. Zhabotinskii, A. N. Zaikin, and A. B. Rovinskii, React. Kinet. Catal. Lett. **20,** 29 (1982).
[3] E. C. Zimmermann, M. Schell, and J. Ross, J. Chem. Phys. **81,** 1327 (1984).
[4] J. Kramer and J. Ross, J. Chem. Phys. **83,** 6234 (1985).
[5] M. Schell and J. Ross, J. Chem. Phys. **85,** 6489 (1986).
[6] J. Weiner, F. W. Schneider, and K. Bar-Eli, J. Phys. Chem. **93,** 2704 (1989).
[7] T. Chevalier, A. Freund, and J. Ross, J. Chem. Phys. **95,** 308 (1991).
[8] P. W. Roesky, S. I. Doumbouya, and F. W. Schneider, J. Phys. Chem., **97,** 398 (1993).
[9] F. W. Schneider, R. Blittersdorf, A. Förster, T. Hauck, D. Lebender, and J. Müller,, J. Phys. Chem. **97,** 12244 (1993).
[10] M. Marek and I. Stuchl, Biophys. Chem. **3,** 241 (1975).
[11] H. Fujii and Y. Sawada, J. Chem. Phys. **69,** 3830 (1978).
[12] a) K. Nakajima and Y. Sawada, J. Chem. Phys. **72,** 2231 (1980). – b) K. Nakajima and Y. Sawada, J. Phys. Soc. Japan **50,** 687 (1981).
[13] I. Stuchl and M. Marek, J. Chem. Phys. **77,** 2956 (1982).
[14] K. Bar-Eli and S. Reuveni, J. Phys. Chem. **89,** 1329 (1985).
[15] M. Boukalouch, J. Elezgaray, A. Arneodo, J. Boissonade, and P. De Kepper, J. Phys. Chem. **91,** 5843 (1987).
[16] M. F. Crowley and I. R. Epstein, J. Phys. Chem. **93,** 2496 (1989).
[17] M. Yoshimoto, K. Yoshikawa, Y. Mori, and I. Hanazaki, Chem. Phys. Lett. **189,** 18 (1992).
[18] S. I. Doumbouya, A. F. Münster, C. J. Doona, and F. W. Schneider, J. Phys. Chem. **97,** 1025 (1993).
[19] S. I. Doumbouya and F. W. Schneider, J. Phys. Chem. **97,** 6945 (1993).
[20] M. Dolnik and I. R. Epstein, J. Chem. Phys. **98,** 1149 (1993).
[21] M. J. B. Hauser and F. W. Schneider, J. Chem. Phys. **100,** 1058 (1994).
[22] a) M. Alamgir and I. R. Epstein, J. Amer. Chem. Soc. **105,** 2500 (1983). – b) J. Maselko, M. Alamgir, and I. R. Epstein, Physica **19D,** 153 (1986).
[23] M. Alamgir and I. R. Epstein, J. Phys. Chem. **88,** 2848 (1984).
[24] J. Maselko and I. R. Epstein, J. Phys. Chem. **88,** 5305 (1984).
[25] a) M. F. Crowley and R. J. Field, in: Nonlinear Phenomena in Chemical Dynamics (C. Vidal and A. Pacault, eds.). Springer, Berlin 1981, p. 147. – b) M. F. Crowley and R. J. Field, in: Lecture Notes in Biomathematics, Nonlinear Oscillations in Biology and Chemistry (H. Othmer, ed.). Springer, Berlin 1986, p. 68. – c) M. F. Crowley and R. J. Field, J. Phys. Chem. **90,** 1907 (1986).
[26] F. W. Schneider, M. J. B. Hauser, and J. Reising, Ber. Bunsenges. Phys. Chem. **97,** 55 (1993).

[27] J. Weiner, R. Holz, F. W. Schneider, and K. Bar-Eli, J. Phys. Chem. **96,** 8915 (1992).
[28] R. Holz and F. W. Schneider, J. Phys. Chem. **97,** 12239 (1993).
[29] K.-P. Zeyer, R. Holz, and F. W. Schneider, Ber. Bunsenges. Phys. Chem. **97,** 1112 (1993).
[30] K. Yoshikawa, K. Fukunaga, and H. Kawakami, Chem. Phys. Lett. **174,** 203 (1990).
[31] M. Yoshimoto, K. Yoshikawa, and Y. Mori, Phys. Rev. **47 E,** 864 (1993).
[32] I. Stuchl and M. Marek, J. Chem. Phys. **77,** 2956 (1982).
[33] a) J.-P. Laplante and T. Erneux, J. Phys. Chem. **96,** 4931 (1992). – b) J.-P. Laplante and T. Erneux, Physica **188 A,** 89 (1992).
[34] A. Hjelmfelt, E. D. Weinberger, and J. Ross, PNAS-USA **88,** 10983 (1991).
[35] A. Hjelmfelt, E. D. Weinberger, and J. Ross, PNAS-USA **89,** 383 (1992).
[36] A. Hjelmfelt and J. Ross, PNAS-USA **89,** 388 (1992).
[37] A. Hjelmfelt and J. Ross, J. Phys. Chem. **97,** 7988 (1993).
[38] A. Hjelmfelt, F. W. Schneider, and J. Ross, Science **260,** 335 (1993).
[39] D. O. Hebb, The Organization of Behaviour, Wiley, New York 1949.
[40] R. M. Noyes, R. J. Field, and R. C. Thompson, J. Amer. Chem. Soc. **93,** 7315 (1971).
[41] a) W. Geiseler, Ber. Bunsenges. Phys. Chem. **86,** 721 (1982). – b) M. Orbàn, P. De Kepper, and I. R. Epstein, J. Amer. Chem. Soc. **104,** 2657 (1982).
[42] B. P. Belousov, Sb. Ref. Radiats Med. za 1958, Medgiz, Moscow 1959, p. 145.
[43] A. M. Zhabotinskii, Biofizika **9,** 306 (1964).
[44] R. Blittersdorf, J. Müller, and F. W. Schneider, J. Chem. Educ., in press.
[45] J. Zupan and J. Gasteiger, Anal. Chim. Acta **248,** 1 (1991).
[46] V. M. Schmidt and W. Vielstich, Ber. Bunsenges. Phys. Chem. **96,** 534 (1992).
[47] P. De Kepper, A. Rossi, and A. Pacault, C. R. Hebd. Acad. Sci. Paris (Ser. C) **283,** 371 (1976).
[48] G. Dechert and F. W. Schneider, J. Phys. Chem. **98,** 3927 (1994).
[49] a) W. Geiseler and H. H. Föllner, Biophys. Chem. **6,** 107 (1977). – b) W. Geiseler and K. Bar-Eli, J. Phys. Chem. **85,** 908 (1981).
[50] a) Z. Noszticzius, W. D. McCormick, and H. L. Swinney, J. Phys. Chem. **91,** 5129 (1987). – b) K. G. Coffman, W. D. McCormick, Z. Noszticzius, R. H. Simoyi, and H. L. Swinney, J. Chem. Phys. **86,** 119 (1987). – c) L. Györgyi, R. J. Field, Z. Noszticzius, W. D. McCormick, and H. L. Swinney, J. Phys. Chem. **96,** 1228 (1992).
[51] D. Lebender and F. W. Schneider, J. Phys. Chem. **98,** 7533 (1994).
[52] E. C. Zimmermann and J. Ross, J. Chem. Phys. **80,** 720 (1984).
[53] M. Orbàn and I. R. Epstein, J. Amer. Chem. Soc. **104,** 5918 (1982).
[54] a) P. De Kepper, I. R. Epstein, and K. Kustin, J. Amer. Chem. Soc. **103,** 6121 (1981). – b) G. A. Papsin, A. Hanna, and K. Showalter, J. Phys. Chem. **85,** 2575 (1981).
[55] R. J. Field and R. M. Noyes, J. Chem. Phys. **60,** 1877 (1974).
[56] L. Györgyi,. T. Turányi, and R. J. Field, J. Phys. Chem. **94,** 7162 (1990).
[57] a) L. Györgyi, S. L. Rempe, and R. J. Field, J. Phys. Chem. **95,** 3159 (1991). – b) L. Györgyi and R. J. Field, J. Phys. Chem. **95,** 6594 (1991).
[58] K. Bar-Eli, J. Phys. Chem. **89,** 2855 (1985).